



Universiteit
Leiden
The Netherlands

Fuel cell electrocatalysis : oxygen reduction on Pt-based nanoparticle catalysts

Vliet, D.F. van der

Citation

Vliet, D. F. van der. (2010, September 21). *Fuel cell electrocatalysis : oxygen reduction on Pt-based nanoparticle catalysts*. Faculty of Science, Leiden University. Retrieved from <https://hdl.handle.net/1887/15968>

Version: Corrected Publisher's Version

License: [Licence agreement concerning inclusion of doctoral thesis in the Institutional Repository of the University of Leiden](#)

Downloaded from: <https://hdl.handle.net/1887/15968>

Note: To cite this publication please use the final published version (if applicable).

Chapter 2

On the Importance of Correcting for the Uncompensated Ohmic Resistance in Model Experiments of the Oxygen Reduction Reaction

When measuring the current due to the oxygen reduction reaction (ORR) and hydrogen oxidation reaction (HOR) on Pt and Pt alloys in aqueous electrolyte, it is important to take care of two major sources of error that are relatively easy to correct for. First, when measuring ORR voltammetry, adsorption processes are superimposed on the current. Second, the system resistance causes an Ohmic drop that may have a profound effect on the measured curves, especially at the higher currents close to the diffusion limiting current. More importantly, we show that it also influences the kinetic part of the potential curve in such a way that the Tafel slope may be determined incorrectly when failing to correct for Ohmic drop. Finally, because electrolyte resistance lowers with increasing temperature, failure to compensate for Ohmic drop may lead to erroneous conclusions about the temperature-dependent activity of a catalyst as well as the corresponding activation energies.

The contents of this chapter have been published: D. van der Vliet, D.S. Strmcnik, C. Wang, V.R. Stamenkovic, N.M. Markovic and M.T.M. Koper, *J. Electroanal. Chem.* **647** (2010) 29

2.1 Introduction

With development of renewable energy and cleaner transportation high on the world's priority list, significant amount of work has been invested in the development of low-temperature polymer electrolyte fuel cells [1]. In order to find better catalysts for these cells, various groups are using the Rotating Disk Electrode (RDE) method to investigate Hydrogen Oxidation (HOR) [2] and Oxygen Reduction (ORR) reactions [3-8], as rotating disk electrodes allow control of the contribution of diffusion limitation to the current [9]. In order to compare the RDE measurements with actual membrane electrode assembly (MEA) fuel cell stack testing, one needs to be aware of all effects that can influence RDE results. This includes the effect of active surface area determination, as explained in [10], adsorbing anions, capacitive currents and solution resistance. In MEA tests it is common practice to compensate the measured ORR activity for IR-drop, but in model RDE experiments it is usually assumed that the electrolyte is sufficiently conductive, and that the currents measured are low enough, to make the contribution of solution resistance negligible.

The effect of the cell geometry on the uncompensated Ohmic drop due to solution resistance has been studied extensively in the past. (See [11-27] and references therein) It is clear from these reports that the geometry and placing of the Luggin-Haber capillary [28] is crucial in reducing measurement errors due to the inhomogeneous current density distribution, Ohmic resistance and shielding of the electrode by the capillary. Since Haber's introduction of the Luggin-Haber capillary, it is well known that the capillary introduces a small, often negligible, Ohmic drop [28]. The classic work of Pontarelli et al [14-17] focuses on the capillary's geometry and placing. They derived that the optimal position of the capillary is through the middle of the electrode from behind [14], but that location is impractical in current cell designs, especially those for single crystal work and rotating disk electrodes. As a good alternative they suggested a closed-top capillary pressed firmly to the electrode, with a tiny opening to the side close to the electrode [14, 15]. Again, this geometry is impractical in RDE experiments, due to the friction it would generate between disk and capillary. This geometry may also disturb diffusion and flow patterns, shielding part of the electrode. Barnartt describes in detail the open Luggin-Haber capillary placed in front of the electrode, at a preferred distance of at least 4 times the capillaries' radius, provided

corrections are made for IR-drop in case of low conductivity or high current densities [18]. This also implies that, ideally, the outer diameter of the capillary is as thin as possible, as wide capillaries are useful only at relatively low current densities in solutions of high conductivity [19]. Furthermore, he notes that in situations of forced convection (such as with a RDE) the capillary tip may alter the hydrodynamic flow. J.E.Harrar et al determined that the optimal position of the capillary is on the line of minimum separation between working and counter electrodes [12].

In this communication, we will show that under rather standard conditions using a popular commercial RDE setup, failure to correct for the Ohmic resistance can impact substantially on the interpretation of kinetic measurements of the ORR. In rotating ring-disk electrodes (RRDE) there will also be an effect of coupling of the potential fields of ring and disk [29], where the individual potential fields of disk and ring are superpositioned thereby causing a coupling resistance. Only disc electrodes were used in this work, so the potential field coupling could not be verified, and will not be further discussed; the interested reader is referred to the detailed work of Dörfel *et al.* [29].

2.2 Experimental

All measurements were performed in HClO₄ solutions, prepared by diluting concentrated perchloric acid (70%, JT Baker Ultrex II) with ultrapure water (Milli-Q gradient; 18.2 MΩ resistivity; 4 ppb total oxidisable carbon) to obtain the desired concentration. Concentrations used are 0.1M, 0.5M and 1.0M HClO₄. The potentiostat used was a computer-controlled Autolab PGSTAT 30 with ECD, Scan Gen, FI20 and FRA (impedance) modules. The electrode assembly consisted of a Pine AFASR rotator with matching Pine electrode shaft. The electrode tips are custom made with disk inserts of Pt and Glassy Carbon of 6 mm diameter. GC disks were polished (Buehler microcloth) to a shiny finish with 0.05μm as finishing polish prior to depositing nanocatalysts.

The 5 nm Pt/C (supplied by TKK, Tokyo, Japan) is deposited by depositing a drop of a sonicated, catalyst-containing suspension onto the GC disk assembled in the collet. In a slow Ar-flow (Airgas, UHP 99.995%) the drop of water is allowed to evaporate, leaving the catalyst deposited on the GC disk. The suspension is made in such a way that 22 μl of the suspension deposited on a 6 mm GC disk gives a

loading of $18 \mu\text{g}_{\text{Pt}} \text{cm}_{\text{disk}}^{-2}$. Polycrystalline Pt disks are annealed by inductive heating before insertion in the collet. The induction heater setup was used to anneal the crystal for 10 minutes at $\sim 1900 \text{ K}$ in an Ar/H₂ atmosphere (Linde Gas, 4.82% hydrogen, high purity).

All cells are of in-house design. A salt bridge connects the main compartment of the cell through the Luggin-Haber Capillary with the reference electrode. A Ag/AgCl reference was used for all experiments; the potentials in this paper are all reported versus the reversible hydrogen electrode (RHE). The position of the Luggin-Haber capillary, with an outer diameter of 2 mm, is as close to the working electrode as possible without generating a shielding effect. This shielding effect appears when the capillary is placed closer to the electrode than 2 times the capillary's outer diameter [18], but for practical purposes can be assumed minor until the distance approaches 1 time the outer diameter of the capillary [15]. Therefore, in our cell, the distance of the Luggin-Haber capillary to the working electrode was typically on the order of 5 to 10 mm, perpendicular to the exposed surface of the working electrode. This is a common location of the capillary in a standard electrochemical cell used by numerous groups [2, 5, 6, 10, 30-35]. The counter electrode was placed in a separate compartment as well, with the opening to the compartment 1 cm to the side of the Luggin-Haber capillary.

Initial blank cyclic voltammetry was measured with the electrode immersed in deoxygenated electrolyte. (Argon; Airgas, research grade plus; 99.9999%) Prior to measuring the oxygen reduction reaction the cell was saturated with oxygen (Airgas, research grade, 99.999%). ORR measurements are recorded with the electrode rotating at 1600 rpm. IR correction during the measurement was done by positive feedback [13, 24]; i.e. the resistance was determined by impedance at a potential which just exhibited diffusion limiting current for the ORR, and was assumed constant during the measurement. A correction voltage proportional to the current was applied during the measurement. Overcompensation for resistance during the measurement of cyclic voltammetry can be quickly noted as the potential will start to oscillate.

2.3 Results and discussion

2.3.1 IR-Drop

The uncompensated resistance can be determined by measuring the high-frequency impedance at operating conditions. Popkurov reported that the uncompensated

resistance can vary during an experiment [24], and may even become a function of the current, *e.g.* through a passivating intermediate that can temporarily increase electrode resistance[24]. This issue can become important especially when research moves away from noble metals as catalysts [4]. Similarly, the resistance can increase in dilute solutions as the diffusion limiting current is approached, due to depletion of charge carriers [23]. In current ORR research, electrolyte concentration usually is 0.1M or higher, with non-passivating (Pt based) catalysts, so the Ohmic resistance is not expected to change during a measurement.

The insert in figure 2.1A shows the Nyquist plot of an impedance measurement on a Pt disk in our assembly. The mean potential was chosen to be within the diffusion limiting regime for the ORR in an oxygen saturated electrolyte to include any resistance induced by the measurement of the ORR. A potential amplitude of 10 mV was applied with frequencies starting at 10kHz and ending with 1 Hz on a logarithmic scale. The figure shows a vertical plot with a minimum in the imaginary part at 2500 Hz. From the real component value of the impedance at the minimum of the Nyquist plot, the Ohmic resistance of the system can be deduced to be 28.5 Ω ., with a possible error of about 0.2 Ω . The value of this resistance is virtually independent of the type of catalyst we use (it deviates by up to 4 Ohm in any given experiment of this kind) and thus is a good representation of a typical value for the solution resistance. Carbon supported nanocatalysts exhibit slightly higher values (an average 34 Ω compared to 28 Ω for polycrystalline Pt) of the resistance due to a small contact resistance in the catalyst layer. Hanging meniscus experiments [34, 35], as generally used for single-crystals, usually have a higher resistance as well due to the longer distance between capillary and electrode. Higher resistance for bead-type single crystals usually does not induce a higher Ohmic drop, unless the surface area of these crystals and the corresponding currents become large, such as with single-crystal disks of 5 [35] mm,6 mm [30, 36] or larger in diameter.

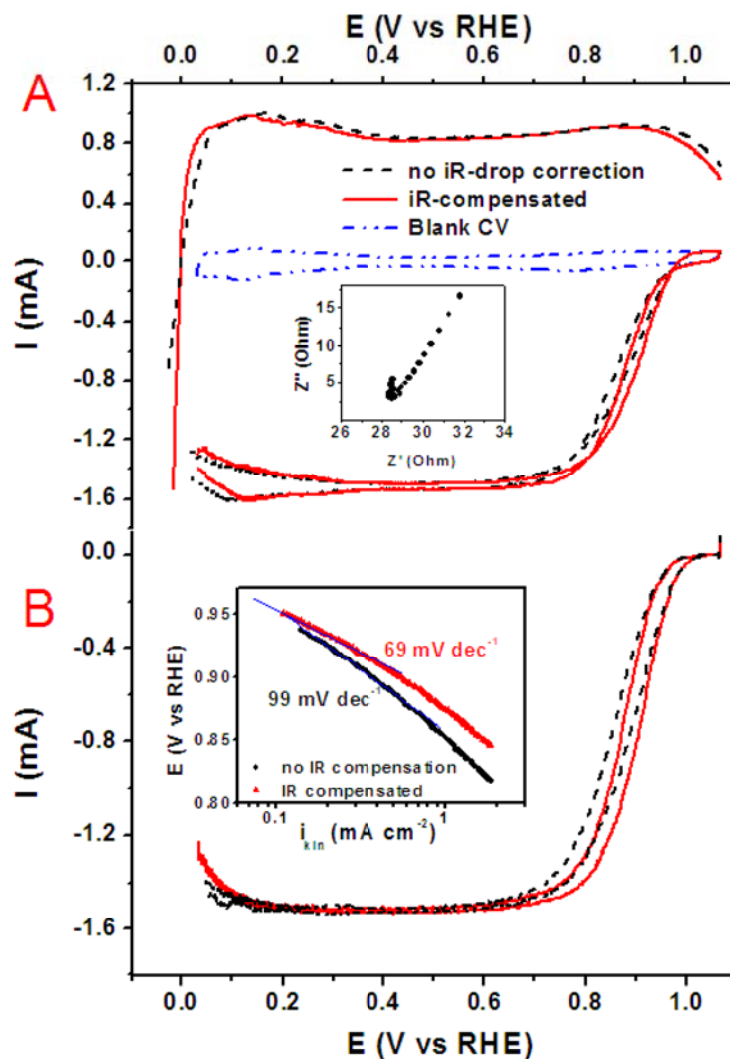


Figure 2.1 A shows the effect of both the resistance and the capacitive currents on the measurement of the HOR and ORR. The black graph shows the measured current as obtained from an experiment without IR drop correction. The red graph shows the current obtained with IR-compensation during the measurement. The blue graph is the blank cyclic voltammogram (no rotation) for this sample. Experimental conditions: Pt/C 5nm, room temperature, 0.1 M HClO₄. Scan rate 20 mV s⁻¹, 1600 rpm for HOR and ORR curves; no rotation for the blank CV. The insert shows the impedance measurement at 0.68V vs. RHE in oxygen-saturated 0.1M HClO₄ at room temperature. Amplitude 0.01 V. Range 1 Hz through 10kHz in a logarithmic scale. Rotation 1600 rpm.

Part B shows the effect of IR-compensation on the measured Tafel slope. Measured in oxygen-saturated 0.1M HClO₄ at room temperature with 1600 rpm rotation.

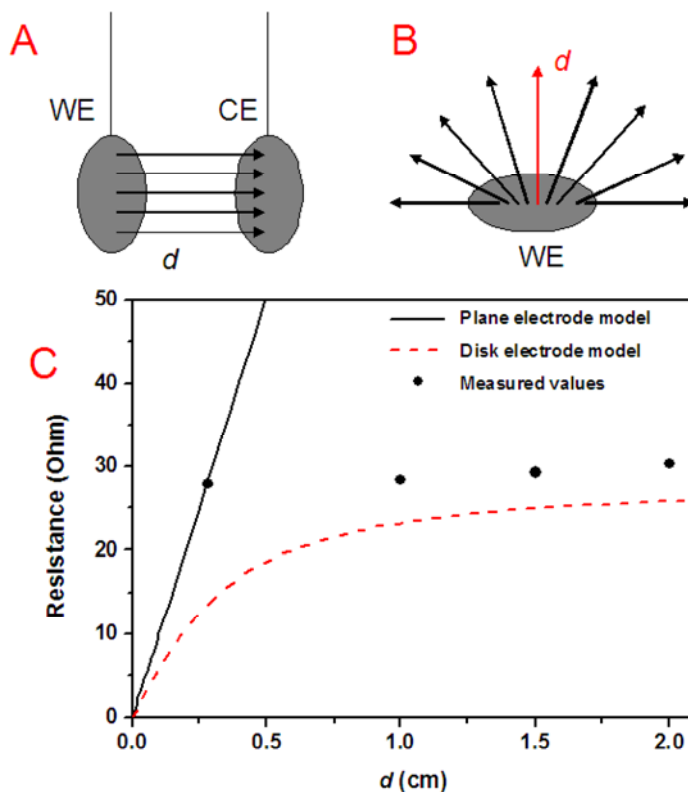


Figure 2.2, A and B show the geometry of the plane electrode model and disk electrode model, respectively. In the plane model the counter electrode is of the same shape and size of the working electrode separated by a finite distance d . The diameter of the disk was chosen to be 6 mm; the planar electrodes were calculated with the same surface area as the disk. The disk model of Newman [11] assumes the counter electrode is at infinity. The arrows in both graphs represent the field lines. Part C shows the apparent resistances predicted by both models and the values retrieved from our experiments in 0.1M HClO₄, equations are listed in the text.

Solution resistance is caused by a combination of low electrolyte concentration and temperature as well as the distance of the Luggin capillary to the surface of the working electrode. However, even if the capillary is brought close to the disk, we find that a significant Ohmic resistance remains, as illustrated in table 2.1. This effect has been observed and calculated before [11, 15, 37], concluding the potential drop increases rapidly until the capillary is brought to about 0.5 mm from the electrode, after which it remains essentially constant. Newman's model [11] shows clearly that, for a 0.1 M copper sulfate solution, even when the probe of the

reference electrode is only half a millimeter from the surface of the electrode, the resistance is by no means negligible. The electrode and cell geometry cause a spherical distribution of current and potential lines, leading to an increase in the apparent resistance which levels off at large distances, as illustrated in figure 2.2. At infinite distance, Newman's geometry gives a resistance of

$$R = 1/(4a\kappa)$$

where a is the radius of the disk and κ is the electrolyte conductivity. For intermediate distances d , the resistance can be estimated according to the procedure outlined by Newman [11]. From his equations for a three dimensional system, a model equation can be derived where the Luggin capillary is placed exactly in line with the electrode surface:

$$R = (2/\kappa\pi) \tan^{-1} (d / a)$$

Figure 2.2 compares, for a 0.1 M HClO₄ solution with an estimated conductivity of $\kappa=0.035$ (ohm cm)⁻¹, [38] the resistance calculated from Newman's model with the resistance between two equally sized disk electrodes:

$$R = d/(\kappa A)$$

where d is the distance between the electrodes and A is their area. This planar model was chosen to mimic the situation where the counter electrode would be small, and the reference measurement placed directly at this counter electrode. From this figure it can be concluded that Newman's model agrees with our experimental situation remarkably well, especially when compared to the planar electrode model. The higher values obtained from experiments can be explained in several ways, such as slightly lower concentration of the electrolyte, lower actual temperature in the cell, shielding effects by the Luggin-Haber capillary at very short distances, or contact resistances in the disk assembly setup. The reason for the discrepancy between model and experiments at short distances of the Luggin capillary is not known precisely, but is assumed to relate to non-distance related resistances, such as contact resistance. As is illustrated in table 2.1 and 2.2, the uncompensated resistance decreases with both increasing temperature and base electrolyte concentration. However, when the concentration is increased from 0.5 to 1.0 M, this does not seem to affect the measured resistance very much; both values are equal

within their standard deviation. Likely the supporting electrolyte is sufficiently abundant that the reduction in resistance due to increased conductivity is very small compared to the residual uncompensated resistive contributions, the exact origin(s) of which remains somewhat elusive. Still, in a model experiment using electrodes of standard size (6 mm diameter), even at such high concentrations and temperatures the contribution of the Ohmic drop needs to be taken into account because the values of resistance will lead to a significant potential drop at the diffusion limiting current for the ORR. For a 28.5 Ω resistance the half-wave potential measured with diffusion limiting current of 1.6 mA is 23 mV lower than the actual potential on the disk, while for a lower IR-drop of 11 Ω it is still a significant shift of 9 mV. These shifts have to be taken into account since they cause a considerable error in the measurement, as will be shown in the next section.

Table 2.1, dependence of Ohmic resistance as measured with impedance on distance of the Luggin capillary from the surface of the electrode. Standard deviations are listed as errors. Electrolyte used was 0.1M HClO₄, impedance spectroscopy was measured at 1600 rpm in oxygen-saturated electrolyte and the solution resistance determined from the minimum in the Nyquist plot.

Distance (mm)	Resistance at 293 K (Ω)	Resistance at 330K (Ω)
2	28.1 \pm 1.0	15.5 \pm 0.8
10	28.5 \pm 0.2	16.5 \pm 0.2
15	29.4 \pm 0.2	18.4 \pm 0.3
20	30.4 \pm 0.8	

Table 2.2, Resistance measured in Impedance measurements for different concentrations of electrolyte. Standard deviations are listed as errors. Impedance spectroscopy was measured at 1600 rpm in oxygen-saturated electrolyte and the solution resistance determined from the minimum in the Nyquist plot.

Concentration HClO ₄ (M)	Resistance at 293 K (Ω)	Resistance at 330K (Ω)
0.1	28.5 \pm 0.2	16.5 \pm 0.2
0.5	11 \pm 1.0	5.5 \pm 0.6
1	11.5 \pm 1.2	7.0 \pm 1.3

2.3.2 Consequences on data interpretation

2.3.2.1 Influence of adsorption processes

The first source of error in determining the activity of a high surface area catalyst for the Oxygen Reduction Reaction (ORR) comes from the current due to adsorption processes at the electrode. Underpotential deposited hydrogen (H_{upd}) and oxide formation processes are taking place during the measurement of the ORR and their current contributions are superimposed on the ORR curve [39]. This is illustrated in figure 2.1A. The figure shows the curve for a high surface area Pt/C-catalyst, deposited on Glassy Carbon (GC) in black, as measured in an oxygen-saturated solution at 1600 rpm with a scan rate of 20 millivolts per second. Also shown in this graph, in blue, is the blank cyclic voltammetry of this sample. The H_{upd} features at potentials lower than 0.4 V are clearly visible in the ORR curve. The oxide plateau at potentials higher than 0.8 V is less obvious, but the oxide reduction peak is again clearly visible at 0.75V in the cathodic sweep. When the scan rate is lowered, the influence of this capacitive current is reduced, but the influence of impurities is simultaneously increased. It is then obvious a more accurate curve will be obtained if the ORR curve can be corrected for the capacitive current from adsorption processes while keeping the scan rate high enough to minimize the effect of impurities. The HOR curves shown in the figure are measured on a similar catalyst and exhibit clear H_{upd} features. The contribution of adsorption on the curve can be neglected if the active surface area is small enough, in case of single crystals for example (see *e.g.* in [40] where such adsorption features are absent). However, for nanocatalysts, high surface area is an intrinsic property of the catalyst and cannot be avoided. Therefore, proper corrections must be applied to eliminate the error induced by adsorption processes. The average contribution to the ORR current from adsorption processes is a function of the surface area and oxide adsorption, ranging from 0.6% for a Pt(111) electrode to 30-50% for high surface area Pt nanoparticles as determined from our experiments. A second way to deal with capacitive currents on high surface area catalysts has been proposed before [41], in which the scan rate can be substantially lowered (to 5 mV s^{-1}) to minimize the contribution of capacitive current. However, this leads to lower activity values due to possible contamination and the hysteresis in the adsorption of oxide containing species.

2.3.2.2 Influence of Ohmic drop

At high current such as the diffusion limiting current in the ORR, the voltammetric features are shifted on the potential axis compared to the blank CV due to Ohmic drop caused by system resistance. This misalignment causes the ORR curve to be distorted when the blank CV is subtracted from the measured ORR curve. A second, more worrying consequence of the Ohmic drop is the significant shift in the steepness of the curve for the ORR. These effects are also illustrated in figure 2.1A: the red curve shows the ORR current as measured with iR compensation, to be compared with the uncompensated curve in black. At low currents the two graphs overlap as the potential shift is negligible there. At high currents however, the compensated curve reflects the true potential as existing at the disk. The adsorption features now line up much better with the blank CV and indeed when the blank CV is subtracted from this curve the resulting ORR curve (figure 2.1B) has a more properly flat diffusion limiting current. The area of interest for studying the oxygen reduction reaction in the potential range of 0.85V to 1.0V exhibits a much steeper curve in case the Ohmic drop is compensated for. This is reflected in the Tafel slope as well. The insert in figure 2.1B shows the effect of iR compensation on the Tafel slope. There is a significant difference in slope between the compensated (69 mV dec^{-1}) and the uncompensated curve (99 mV dec^{-1}). As the Tafel slope is used to obtain information on the reaction kinetics, measuring the wrong slope can lead to wrong conclusions. The dependence of the HOR on Ohmic drop is shown in figure 2.1A. The steepness of the curve changes dramatically with iR drop correction. This again causes Tafel slopes to be inaccurate. Perhaps the most striking example of this is the comparison of the measured Tafel slopes with measurements in the membrane electrode assembly (MEA) [41], where the Tafel slope is found to be straight, due to the fact that in MEA's the Ohmic drop is compensated for, the mass transport is much faster, and there is no influence of capacitive currents as the current densities are measured in steady-state rather than sweeps. Furthermore, the absolute value of the kinetic current (i_{kin}), often used as an indication of the catalysts activity increases significantly when Ohmic drop is applied appropriately; see table 2.3. Thus in order to be able to compare data from different research groups it is important to compensate for Ohmic drop, lest the resistance is compared rather than the activity.

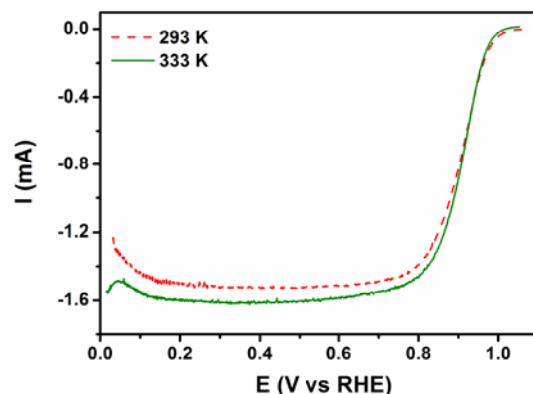


Figure 2.3. ORR dependence on temperature for the measurement with IR-drop compensation. The red curve shows the measurement at 293K; the green one shows the measurement at 333K. Experimental Conditions: Pt/C 5 nm, 0.1 M HClO₄, scan rate 20 mV s⁻¹, rotation 1600 rpm.

Another unfortunate side effect of solution resistance is its dependence on the temperature. Table 2.2 shows that when the temperature of the cell is increased from room temperature to 330K the measured iR drop almost halves compared to the value at 293K. Figure 2.3 shows the iR compensated curves for an ORR measurement on the Pt/C high surface area catalyst. When the results for the ORR activity of these catalysts are together analyzed, the results of which are given in table 2.3 and 2.4, one concludes that when iR compensation is not applied, the difference between $E_{1/2}$ of the room temperature experiment and the measurement at elevated temperatures is smaller than when iR compensation is properly applied (table 2.4). The kinetic current values in table 2.3 are given in mA per cm² electrochemical surface area. This area was determined in the same way as reported before by Mayrhofer *et al.* [10] The uncompensated data in table 2.3 matches our group's previous data [10, 42], the reported activities by other groups [7, 43, 44] and previously published benchmarks [41] almost perfectly. Also, as can be seen from the value of the kinetic current at 925 mV, it is easy to draw wrong conclusions about which temperature has the highest activity for the ORR. In the uncorrected data, the elevated temperatures seem to be more active, whereas with proper correction the data shows that such is not the case. This observation also means that when we are looking in literature for data on ORR measurements with temperature dependence, we have to be very careful with interpreting such data

when it is obtained without Ohmic drop compensation. Small apparent activation of catalysts at elevated temperatures in those data may be not much more than an observation of the lower cell resistance. In addition to this, measurements of activation energies with bigger electrodes have to be very carefully compensated for Ohmic drop. As the resistance decreases with increasing temperature it will change the slope of an Arrhenius plot (log current versus the reciprocal of the absolute temperature), and thus it will cause the measured apparent activation energy to be unrepresentative of the kinetic process one is trying to measure.

Table 2.3. Kinetic current density values for the ORR of a Pt/C 5 nm nanocatalyst. The kinetic current densities were obtained from the positive-going ORR curve, which was first corrected for capacitive currents, and consecutively corrected for mass transport.

Potential (mV vs. RHE)	No IR-drop correction		IR-compensated	
	I_{kin} at 293K (mA cm _{Pt} ⁻²)	I_{kin} at 333K (mA cm _{Pt} ⁻²)	I_{kin} at 293K (mA cm _{Pt} ⁻²)	I_{kin} at 333K (mA cm _{Pt} ⁻²)
900	0.37	0.45	0.54	0.6
925	0.20	0.22	0.27	0.27
950	0.097	0.095	0.115	0.105

Table 2.4, half-wave potential ($E_{1/2}$) dependence on the Ohmic drop.

	$E_{1/2}$ at 293K (mV)	$E_{1/2}$ at 333K (mV)
No IR-drop correction	889	897
IR-compensated	905	906

2.4 Conclusion and Recommendations

In this paper, we have argued that without proper correction for 1) adsorption processes and 2) IR compensation, the values for kinetic currents of model electrocatalysts in model experimental setups may be incorrect and may lead to misleading results in the comparison of catalysts. Although we realize that this conclusion appears “old news”, the examples given in this paper illustrate the dramatic influence of proper IR compensation, especially for temperature dependent measurements, that is nevertheless often disregarded.

Especially on high surface area catalysts the contribution from the oxide adsorption process at potentials of 0.8V and higher will be significant (up to 50%) and failing to correct for this makes comparisons between catalysts with different surface areas or different shapes of said oxide plateau impossible.

Ohmic drop compensation is even more important as the resistance of the solution will not always be exactly the same, especially when comparing between different setups and electrolyte concentrations and temperatures. In order to make a meaningful comparison between ORR catalysts measured in different environments, indeed even different research groups, one needs to be sure the actual reaction activity is compared and not the difference in iR drop between the different measurements.

Positive feedback is a relatively easy way of correcting for most of the resistance problem. This correction will not only make comparisons between catalysts more meaningful, it will simultaneously ensure that Tafel slopes are correct. Finally, another important advantage of properly correcting for Ohmic drop lies in the fact that conclusions derived from measurements at different temperatures will actually represent the influence of temperature on reaction kinetics, rather than on changed electrolyte conductivity. This includes proper determination of temperature dependence of the kinetic activity for the ORR, as well as apparent activation energies measured and calculated for a plethora of different reactions.

Summarizing, the problem of Ohmic drop is clearly nothing new, but is still often overlooked, or often assumed negligible, even though it is of significant influence. We recommend scrutinizing very carefully what influence this IR drop as well as adsorption processes have in an experiment, and to duly compensate for them to ensure a valid evaluation of catalysts in electrocatalysis.

References

- [1] W. Vielstich, A. Lamm, and H. A. Gasteiger, eds., Handbook of Fuel Cells: Fundamentals, Technology, Applications, Wiley, 2003.
- [2] H. A. Gasteiger, N. M. Markovic, and P. N. Ross, *Journal of Physical Chemistry*. 99 (1995) 8290.
- [3] F. Gloaguen, F. Andolfatto, R. Durand, and P. Ozil, *Journal of Applied Electrochemistry*. 24 (1994) 863.
- [4] D. Susac, A. Sode, L. Zhu, P. C. Wong, M. Teo, D. Bizzotto, K. A. R. Mitchell, R. R. Parsons, and S. A. Campbell, *Journal of Physical Chemistry B*. 110 (2006) 10762.
- [5] W. Chen, J. M. Kim, S. H. Sun, and S. W. Chen, *Journal of Physical Chemistry C*. 112 (2008) 3891.

- [6] A. Sode, W. Li, Y. G. Yang, P. C. Wong, E. Gyenge, K. A. R. Mitchell, and D. Bizzotto, *Journal of Physical Chemistry B*. 110 (2006) 8715.
- [7] S. Koh and P. Strasser, *Journal of the American Chemical Society*. 129 (2007) 12624.
- [8] N. M. Markovic, H. A. Gasteiger, and P. N. Ross, *Journal of Physical Chemistry*. 99 (1995) 3411.
- [9] Z. Galus, C. Olson, H. Y. Lee, and R. N. Adams, *Analytical Chemistry*. 34 (1962) 164.
- [10] K. J. J. Mayrhofer, D. Strmcnik, B. B. Blizanac, V. Stamenkovic, M. Arenz, and N. M. Markovic, *Electrochimica Acta*. 53 (2008) 3181.
- [11] J. Newman, *Journal of the Electrochemical Society*. 113 (1966) 501.
- [12] J. E. Harrar and I. Shain, *Analytical Chemistry*. 38 (1966) 1148.
- [13] P. X. He and L. R. Faulkner, *Analytical Chemistry*. 58 (1986) 517.
- [14] R. Piontelli, G. Bianchi, and R. Aletti, *Zeitschrift Fur Elektrochemie*. 56 (1952) 84.
- [15] R. Piontelli, G. Bianchi, U. Bertocci, C. Guerci, and B. Rivolta, *Zeitschrift Fur Elektrochemie*. 58 (1954) 54.
- [16] R. Piontelli, U. Bertocci, G. Bianchi, C. Guerci, and G. Poli, *Zeitschrift Fur Elektrochemie*. 58 (1954) 86.
- [17] R. Piontelli, B. Rivolta, and G. Montanelli, *Zeitschrift Fur Elektrochemie*. 59 (1955) 64.
- [18] S. Barnartt, *Journal of the Electrochemical Society*. 99 (1952) 549.
- [19] S. Barnartt, *Journal of the Electrochemical Society*. 108 (1961) 102.
- [20] G. L. Booman and W. B. Holbrook, *Analytical Chemistry*. 35 (1963) 1793.
- [21] W. B. Schaap and P. S. Mckinney, *Analytical Chemistry*. 36 (1964) 1251.
- [22] W. T. De Vries and E. Van Dalen, *Journal of Electroanalytical Chemistry*. 12 (1966) 9.
- [23] M. Hayes, A. T. Kuhn, and W. Patefield, *Journal of Power Sources*. 2 (1977) 121.
- [24] G. S. Popkurov, *Journal of Electroanalytical Chemistry*. 359 (1993) 97.
- [25] J. C. Myland and K. B. Oldham, *Journal of Electroanalytical Chemistry*. 347 (1993) 49.
- [26] J. O. Bockris, *Chemical Reviews*. 43 (1948) 525.
- [27] R. S. Nicholson, *Analytical Chemistry*. 37 (1965) 667.
- [28] F. Haber, *Zeitschrift Für Physikalische Chemie*. 32 (1900) 193.
- [29] C. Dorfel, D. Rahner, and W. Forker, *Journal of Electroanalytical Chemistry*. 107 (1980) 257.
- [30] V. R. Stamenkovic, B. Fowler, B. S. Mun, G. F. Wang, P. N. Ross, C. A. Lucas, and N. M. Markovic, *Science*. 315 (2007) 493.
- [31] S. Koh, M. F. Toney, and P. Strasser, *Electrochimica Acta*. 52 (2007) 2765.
- [32] A. Bonakdarpour, K. Stevens, G. D. Vernstrom, R. Atanasoski, A. K. Schmoekkel, M. K. Debe, and J. R. Dahn, *Electrochimica Acta*. 53 (2007) 688.
- [33] T. Toda, H. Igarashi, and M. Watanabe, *Journal of Electroanalytical Chemistry*. 460 (1999) 258.
- [34] J. Barber, S. Morin, and B. E. Conway, *Journal of Electroanalytical Chemistry*. 446 (1998) 125.
- [35] J. Perez, H. M. Villullas, and E. R. Gonzalez, *Journal of Electroanalytical Chemistry*. 435 (1997) 179.
- [36] T. J. Schmidt, P. N. Ross, and N. M. Markovic, *Journal of Electroanalytical Chemistry*. 524-525 (2002) 252.

- [37] J. O. Bockris and A. M. Azzam, *Transactions of the Faraday Society*. 48 (1952) 145.
- [38] R. C. Weast and M. J. Astle, eds., *CRC Handbook of Chemistry and Physics*, CRC Press Inc., Boca Raton, FL, USA, 1982-1983.
- [39] D. S. Strmcnik, P. Rebec, M. Gaberscek, D. Tripkovic, V. Stamenkovic, C. Lucas, and N. M. Markovic, *Journal of Physical Chemistry C*. 111 (2007) 18672.
- [40] D. Strmcnik, D. Tripkovic, D. van der Vliet, V. Stamenkovic, and N. M. Markovic, *Electrochemistry Communications*. 10 (2008) 1602.
- [41] H. A. Gasteiger, S. S. Kocha, B. Sompalli, and F. T. Wagner, *Applied Catalysis B-Environmental*. 56 (2005) 9.
- [42] K. J. J. Mayrhofer, B. B. Blizanac, M. Arenz, V. R. Stamenkovic, P. N. Ross, and N. M. Markovic, *Journal of Physical Chemistry B*. 109 (2005) 14433.
- [43] J. B. Wu, J. L. Zhang, Z. M. Peng, S. C. Yang, F. T. Wagner, and H. Yang, *Journal of the American Chemical Society*. 132 (2010) 4984.
- [44] S. Chen, P. J. Ferreira, W. C. Sheng, N. Yabuuchi, L. F. Allard, and Y. Shao-Horn, *Journal of the American Chemical Society*. 130 (2008) 13818.